

Generalized Relative Neighborhood Graph (GRNG) for Similarity Search^{*}

Cole Foster, Berk Sevilimis, and Benjamin Kimia

Brown University, Providence RI 02912, USA
{cole_foster,benjamin_kimia}@brown.edu

Abstract. Similarity search is a fundamental building block for information retrieval on a variety of datasets. The notion of a neighbor is often based on binary considerations, such as the k nearest neighbors. However, considering that data is often organized as a manifold with low intrinsic dimension, the notion of a neighbor must recognize higher-order relationship, to capture neighbors in all directions. Proximity graphs, such as the Relative Neighbor Graphs (RNG), use trinary relationships which capture the notion of direction and have been successfully used in a number of applications. However, the current algorithms for computing the RNG, despite widespread use, are approximate and not scalable. This paper proposes a novel type of graph, the Generalized Relative Neighborhood Graph (GRNG) for use in a pivot layer that then guides the efficient and exact construction of the RNG of a set of exemplars. It also shows how to extend this to a multi-layer hierarchy which significantly improves over the state-of-the-art methods which can only construct an approximate RNG.

Keywords: Generalized Relative Neighborhood Graph · Incremental Index Construction · Scalable Search

1 Introduction

The vast majority of generated data in our society is now in digital form. The data representation has evolved beyond numbers and strings to complex objects. Organization and retrieval have likewise evolved from cosine similarity in vector spaces through inverted files (Google, Yahoo, Microsoft, etc.), to either embedding complex objects in Euclidean spaces or to the use of similarity metrics. The task of similarity search, namely, finding the “neighbors” of a given query based on similarity, is a fundamental building block in application domains such as information retrieval (web search engines, e-commerce, museum collections, medical image processing), pattern recognition, data mining, machine learning, and recommendation systems.

Formally, consider the set of all objects of interest \mathcal{X} , hereby referred to as points, data points, or exemplars, and let $\mathcal{S} \subset \mathcal{X}$ be a dataset containing N such objects. Let $d(x, y)$ denote a metric that captures the distance, or the extent of dissimilarity, between $x, y \in \mathcal{X}$. It is important to note that the focus of this work is search in a *metric space*, *i.e.*, where the metric satisfies $d(x, y) = 0 \Leftrightarrow x = y$, $d(x, y) = d(y, x)$, and $d(x, z) \leq d(x, y) + d(y, z)$. Some approaches first embed the metric space in a Euclidean space, such as hashing, quantization, CNN, *etc.*, but

^{*} The support of NSF award 1910530 is gratefully acknowledged.

this can distort the relative distances: this paper aims to define a hierarchical index structure for a metric space and use it for similarity search.

In absence of an embedding space, notions of proximity, neighborhood, and topology are constructed through a graph. The two most popular graphs are the k NN graph [4], where each element is connected to its k nearest neighbors, and the Minimum Spanning Tree (MST) which is the spanning tree (connected tree involving all nodes) that has the least cumulative sum of distances over all links. However, the k NN graph is not necessarily connected: in clustered data, the k closest neighbors may be to one side of an element so that the k NN may not faithfully represent the spatial neighborhood, Figure 1(c), in that only connections to one side are represented. Connectivity can be achieved with a sufficiently high choice of k , but that is at the expense of over-representing neighboring connections elsewhere, Figure 2(a,b). A much better choice that captures the spatial layout in all “directions” is using a class of *proximity graphs*, which define a spatial neighborhood for every pair of points x_1 and x_2 , and a connection is made if this spatial neighborhood does not contain any other points (also referred to as *empty-neighborhood graphs*). For example, a *Gabriel Graph* (GG) [7] connects two points $x_1, x_2 \in \mathcal{S}$ if the sphere with diameter x_1x_2 is empty, or $d^2(x_3, x_1) + d^2(x_3, x_2) \geq d^2(x_1, x_2)$, $\forall x_3 \in \mathcal{S}$. Another important example is the *Relative Neighborhood Graph* (RNG) [11,20] which connects x_1 and $x_2 \in \mathcal{S}$ if the *lune*(x_1, x_2), namely, the intersection of the two spheres of radius x_1x_2 through centers x_1 and x_2 , is empty, *i.e.*, if

$$\max(d(x_3, x_1), d(x_3, x_2)) \geq d(x_1, x_2), \forall x_3 \in \mathcal{S}. \quad (1)$$

Other proximity graphs of interest include the Half-Space Graph (HSG), which is a superset of RNG and a t -spanner [1], the *Delaunay Triangulation* (DT) graph [3], and the β -skeleton graph [13]. Proximity graphs generally require consideration of all members x_3 of S for each pair (x_1, x_2) of S , and as such require $O(N^3)$ for naive construction. Note that $1\text{NN} \subset \text{MST} \subset \text{RNG} \subset \text{GG} \subset \text{DT}$. See Figure 1.

We adopt the use of RNG not only because (i) it is connected, but also because (ii) it is parameter free, in contrast to k NN, where k has to be specified, Tellez [19] where “b” and “t” have to be defined, and NSG [6] where “R” has to be defined, also (iii) the RNG is a relatively sparse graph, unlike other choices presented in Figure

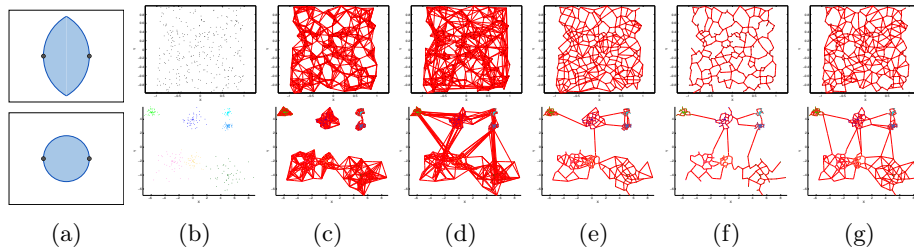


Fig. 1: (a) (top) Two points have an RNG connection if the "lune" between them does not contain other points. (bottom) Two points have a Gabriel Graph (GG) connection if the circle with the line segment between the points as diameter is empty. A comparison of graphs for representing both uniformly distributed points in \mathcal{R}^2 (top) and clustered data (bottom). (b) Points in 2D, (c) k NN, $k=8$, (d) Tellez [19] $b=4$, $t=4$, (e) NSG [6], $R=8$, (f) RNG, and (g) GG.

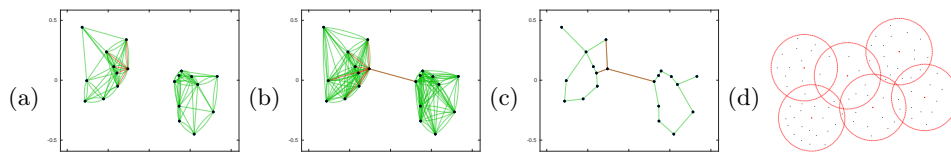


Fig. 2: The k NN connectivity is only based on distance between two elements and not on geometric distribution, (a) $k=5$ and (b) $k=8$. In contrast, the RNG (c) captures local geometry without regard to distance and requires no parameters. (d) Pivots (red dots) and associated radii define a pivot domain (red discs).

1. Figure 10(e) shows the out degree of RNG is small and grows very slowly with intrinsic dimension.

There are a large number of applications that use the RNG. The RNG is used in graph-based visualization of large image datasets for browsing and interactive exploration and is viewed as the smallest proximity graph that captures the local structure of the manifold [14,15,16]. In urban planning theory, RNGs have been used to model topographical arrangements of cities and the road networks. In internet networks, Escalante *et al.* [5] found that broadcasting over the RNG network is superior to blind flooding. De Vries *et al.* [21] propose to use the RNG to reveal related dynamics of page-level social media metrics. Han *et al.* [10] aims to improve the efficiency of a Support Vector Machine (SVM) classifier by using the RNG to extract probable support vectors from all the training samples. Goto *et al.* [8] use the RNG to reduce a training dataset consisting of handwritten digits to 10% of its original size. A related and more recent area is the selection of training data for Convolutional Neural Networks (CNNs) where the RNG is used to reduce the underlying redundancy of the dataset [17].

Despite such widespread use of RNG, there is not a large literature on efficient construction of the RNG in metric spaces. In Euclidean spaces, the notions of angle and direction allow for an efficient implementation, *e.g.*, an $O(N \log N)$ for N points in \mathcal{R}^2 [18], an $O(N)$ for uniformly distributed points in a rectangle [12], and an $O(N^2)$ for higher dimensions [18]. The construction of the RNG for general metric spaces, however, has been more challenging, limited to two groups of papers. First, Hacid *et al.* [9] propose an approximate incremental RNG construction algorithm for data mining and visualization purposes. This approximate construction defines the set of potential RNG neighbors and the set of potentially invalidated RNG links by only considering dataset items that fall within a hypersphere around the query's nearest neighbor, where its radius is proportional to the distance from the query to its nearest neighbor plus the distance from the nearest neighbor to its furthest RNG neighbor. Second, Rayar *et al.* [14] proposed an improvement over Hacid's algorithm by defining the set of potentially invalidated RNG links by the L^{th} edge neighbors of the query. While both these methods work in any metric space and provide significant speed-up over naive construction, they are *approximate* and thus lose all guarantees provided by the RNG, and make a significant number of errors, as will be shown by Table 4.

The main computational challenge in searching metric spaces is to reduce the number of distance computations which are expensive, in contrast to vector spaces where the aim is to reduce I/O. The general approach is to build an *index* which

effectively builds a set of equivalence classes so that some classes can be discarded leaving others to be exhaustively searched, either through compact partitioning or through pivoting [2]. The notion of a *pivot* arises as a way to capture a group of exemplars. Define the *pivot domain*, Figure 2(d), \mathcal{D} of pivot p_i and domain radius r_i as,

$$\mathcal{D}(p_i, r_i) = \{x \in \mathcal{S} \mid d(x, p_i) \leq r_i\}. \quad (2)$$

While pivots do not necessarily need to be members of \mathcal{S} , in a metric space which cannot generate new members a pivot is also an exemplar/data point. A sufficient number of pivots $\mathcal{P} = \{p_1, p_2, \dots, p_M\} \subset \mathcal{S}$ are required to cover \mathcal{S} , *i.e.*, $\mathcal{S} = \bigcup_{i=1}^M \mathcal{D}(p_i, r_i)$.

Observe that the knowledge of $d(x, p_i)$ bounds $d(x, y)$ for $y \in S_i$ as $d(y, p_i) - r_i \leq d(x, y) \leq d(y, p_i) + r_i$ using the triangle inequality. In the absence of an embedding Euclidean structure the triangle inequality is the only constraint available for relative ranking of distances between triplets of points. For simplicity we take $r_i = r$ in this paper.

The key aim of this paper is to design a hierarchical index that allows for the construction of the exact RNG and allows for efficient search of RNG neighbors of a given query Q . The contribution of the paper is to show that in a two-layer configuration of pivots and exemplars (data points) a novel graph structure, the Generalized Relative Neighborhood Graph (GRNG), allows for efficient and exact construction of RNG of the data points. Note that the RNG is a special case of GRNG when its parameter $r = 0$. In addition, we also show that the GRNG of any coarse-layer of pivots can guide the exact construction of the GRNG of any fine-layer pivots. This allows for a highly efficient, scalable, hierarchical construction involving multiple layers (for a dataset of 26 million points in \mathcal{R}^2 ten layers is optimal []). Observe that construction is incremental so that the index can be dynamically updated. Given a query, a search process locates it in the hierarchy by examining the coarsest layers, discarding all the exemplar domains for a majority of the pivots and then moving on to the next layers where finer-scale pivot children of a few select coarse-scale pivots need to be considered. This process is then repeated to the lowest layer, the exemplar domain. The query is then located in the RNG and its RNG neighbors are identified. The search process is highly efficient and logarithmic in the number of exemplars in all dimensions, Figure 10(b,d).

The incremental construction of the index relies on the search component described above to locate the query in each layer, but in addition, in each layer new connections must be made and existing connections must be validated. The construction is done off-line in contrast to search which is typically done on-line. While the construction is exponential in both the number of exemplars and dimensions for uniformly distributed data, for practical applications where the data is clustered, the construction cost behaves much better. The experimental results summarized in Table 4 show that while our method gives the exact RNG neighbors, it is substantially faster in both constructing the RNG and in searching it.

2 Incremental Construction of the RNG

The incremental approach to constructing RNG assumes that $\text{RNG}(\mathcal{S})$ is available and computes $\text{RNG}(\mathcal{S} \cup Q)$ from it. The query Q is the newest element: *(i) Localize Q within \mathcal{S}* : finding the RNG Neighbors of Q . The naive approach would consider for all $x_i \in \mathcal{S}$ whether $\exists x_j \in \text{lune}(Q, x_i)$; all x_i with empty lunes are RNG neighbors of Q . Note that this involves $O(N^2)$ operations where $N = |\mathcal{S}|$, and this is clearly not scalable, and *(ii) Adding Q to the dataset*: When the task is search, the first step finds the RNG neighbors. If Q needs to be added, additionally all pairs of existing links between x_i and x_j need to be validated, whether $Q \in \text{lune}(x_i, x_j)$ in which case x_i and x_j are no longer RNG neighbors. This operation is on the order of $O(\alpha N)$ where α is the average out degree of the RNG, typically a small number. Thus, the localization step is significantly more computationally intensive than the validation step.

The remedy to indexing complexity is organization. Specifically, when exemplar groups are represented by pivots, many inferences can take place at the level of pivot domains without computing distances between Q and exemplars. The basic idea in this paper is to construct conditions on pivots that have implications for efficient incremental construction of RNG of exemplars. This is organized in seven stages: *i)* In Stages I,II, and III entire pivot domains $\mathcal{D}(p_i, r_i)$ or a significant number of exemplars x_i are discarded from considering RNG neighbor relations with Q by just measuring $d(Q, p_i)$; *ii)* Stages IV,V, and VI: pivots are used in invalidating potential RNG links with the remaining exemplars; *iii)* Stage VII: pivots are used to exclude entire domains during the RNG validation process of existing links. What relationship between p_i and p_j can prevent the formation of a RNG link between x_i and x_j ?

Theorem 1. Consider exemplars $x_i \in \mathcal{D}(p_i, r_i)$ and $x_j \in \mathcal{D}(p_j, r_j)$. Then

$$\begin{cases} d(p_k, p_i) < d(p_i, p_j) - (2r_i + r_j) \\ d(p_k, p_j) < d(p_i, p_j) - (r_i + 2r_j) \end{cases} \Rightarrow \max(d(p_k, x_i), d(p_k, x_j)) < d(x_i, x_j) \quad (3)$$

Proof. Equation 3 requires that $d(p_k, x_i) < d(x_i, x_j)$ and $d(p_k, x_j) < d(x_i, x_j)$, which can be established by a two-fold application of the triangle inequality, first relating $d(p_k, x_i)$ and $d(p_k, x_j)$ to $d(p_k, p_i)$ and then to $d(p_k, p_j)$, respectively,

$$\begin{cases} d(p_k, p_i) - r_i \leq d(p_k, p_i) - d(p_i, x_i) \leq d(p_k, x_i) \leq d(p_k, p_i) + d(p_i, x_i) \leq d(p_k, p_i) + r_i & (4a) \\ d(p_k, p_j) - r_j \leq d(p_k, p_j) - d(p_j, x_j) \leq d(p_k, x_j) \leq d(p_k, p_j) + d(p_j, x_j) \leq d(p_k, p_j) + r_j. & (4b) \end{cases}$$

Similarly, $d(x_i, x_j)$ can be related to $d(p_i, p_j)$ by applying the triangle inequality twice:

$$d(p_i, p_j) - r_j - r_i \leq d(p_i, x_j) - r_i \leq d(p_i, x_j) - d(p_i, x_i) \leq d(x_i, x_j) \leq d(p_i, x_j) + d(p_i, x_i) \leq d(p_i, x_j) + r_i \leq d(p_i, p_j) + r_j + r_i. \quad (5)$$

Thus, if the right side of Equation 4a is smaller than the left side of Equation 5, *i.e.*,

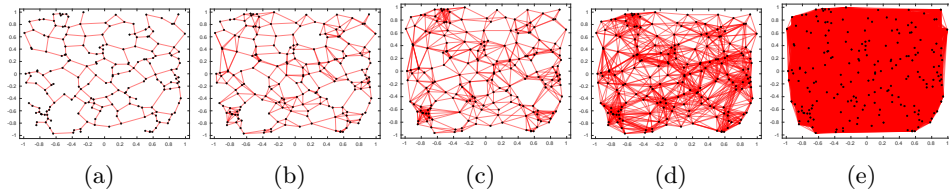


Fig. 3: GRNG of a set of 200 points in $[-1, 1]^2$ where all $r_i = r$ and for different selection of r : (a) $r = 0$, (b) $r = 0.01$, (c) $r = 0.02$, (d) $r = 0.04$, and (e) $r = 0.419$. When r exceeds $\frac{1}{6}$ the maximum distance between points it is the complete graph (e).

$$d(p_k, p_i) + r_i < d(p_i, p_j) - r_j - r_i, \quad (6)$$

then combining Equations 4a, and 5 gives

$$d(p_k, x_i) < d(x_i, x_j). \quad (7)$$

Similarly, if we have

$$d(p_k, p_j) + r_j < d(p_i, p_j) - r_j - r_i, \quad (8)$$

then combining Equations 4b, and 5 gives

$$d(p_k, x_j) < d(x_i, x_j). \quad (9)$$

Thus, when Equations 6 and 8 hold, or stated differently when

$$\begin{cases} d(p_k, p_i) < d(p_i, p_j) - 2r_i - r_j & (10a) \\ d(p_k, p_j) < d(p_i, p_j) - r_i - 2r_j, & (10b) \end{cases}$$

then $\max(d(p_k, x_i), d(p_k, x_j)) < d(x_i, x_j)$, *i.e.*, an RNG connection cannot exist between x_i and x_j . \square

Theorem 1 states that a pivot p_k that falls in a lune defined by the intersection of the sphere at p_i with radius $d(p_i, p_j) - (2r_i + r_j)$ and the sphere at p_j with radius $d(p_i, p_j) - (r_i + 2r_j)$ also falls in the RNG lune of x_i and x_j , thereby invalidating the potential RNG link between x_i and x_j , *without computing* $d(p_k, x_i)$ and $d(p_k, x_j)$! This is a proximity relationship between p_i, p_j , and p_k , which effectively defines a novel type of graph.

Definition 1. (*Generalized Relative Neighborhood Graph (GRNG)*): Two pivots $p_i, p_j \in \mathcal{P}$ have a GRNG link iff no pivots $p_k \in \mathcal{P}$ can be found inside the generalized lune defined by,

$$\begin{cases} d(p_k, p_i) < d(p_i, p_j) - (2r_i + r_j) & (11a) \\ d(p_k, p_j) < d(p_i, p_j) - (r_i + 2r_j). & (11b) \end{cases}$$

Observe that $\text{GRNG}(\mathcal{P})$ is just the RNG when $r_i = 0, \forall i$, thus it is a generalization of it, Figure 3. Also, note that $\text{GRNG}(\mathcal{P})$ is a superset of $\text{RNG}(\mathcal{P})$ since $\text{lune}(p_i, p_j)$ is larger than the generalized-lune(p_i, p_j), abbreviated as G-lune(p_i, p_j). This implies that the larger r_i and r_j are, the denser the graph is, until it is effectively the complete graph. This places a constraint on how large r_i and r_j can be. Furthermore, it is easy to show that $\text{GRNG}(\mathcal{P})$ is a connected graph. In practice, all pivots share the same uniform radius, *i.e.*, $r_i = r, \forall i$. The single parameter r is the minimum for which the union of all pivot domains cover \mathcal{S} . Thus, the number of pivots M and r are inversely related. In what follows $d(Q, p_i), i = 1, 2, \dots, M$ is computed.

Stage I: Pivot-Pivot Interaction: The most important implication of the $\text{GRNG}(\mathcal{P})$ via Theorem 1, is that a lack of a GRNG link between p_i and p_j invalidates all potential links between their constituents. Stage I therefore begins by locating the pivot parents of Q in \mathcal{P} , Equation 2. If Q has no parents, Q is added to the set of pivots \mathcal{P} and $\text{GRNG}(\mathcal{P})$ is updated. Otherwise, Q can only have RNG links with the common GRNG neighbors of *all* of Q 's parents. See Figure 5.

Stage II: Query-Pivot Interaction: Stage I removes entire pivot domains from interacting with Q , namely, those exemplars in the domain of pivots that do not have GRNG links to *all* parents of Q . Note, however, that the GRNG lune is significantly reduced in size due to the increased radii, in comparison with RNG, *i.e.*, by $2r_i + r_j, r_i + 2r_j$ on each side. This stage enlarges the G-lune by considering Q itself as a virtual parent pivot with $r_Q = 0$.

Proposition 1. *If p_k is in the G-lune of (p_i, r_i) and $(Q, r_Q = 0)$, *i.e.*,*

$$\begin{cases} d(Q, p_k) < d(Q, p_i) - r_i & (12a) \\ d(p_i, p_k) < d(Q, p_i) - 2r_i. & (12b) \end{cases}$$

*Then, p_k is also in the RNG lune $(Q, x_i) \forall x_i \in \mathcal{D}(p_i, r_i)$, thereby invalidating it, *i.e.*, $\max(d(p_k, Q), d(p_k, x_i)) < d(Q, x_i)$.*

Proof. Apply Theorem 1 with $p_i = Q, p_j = p_j$ and $p_k = p_k$ with radii $r_i = r_Q = 0$. The conditions of the theorem is then

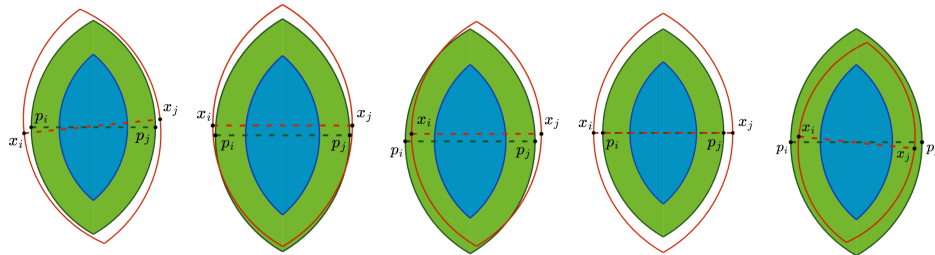


Fig. 4: A few examples illustrating the similarity between the lune (x_i, x_j) and the lune (p_i, p_j), where x_i and x_j are both fairly close to p_i and p_j , respectively, relative to $d(x_i, x_j)$ but otherwise unconstrained. Lune(x_i, x_j) is shown in red, lune(p_i, p_j) is shown in blue, and G-lune(p_i, p_j) is shown in green. Note how much smaller the generalized lune is compared to the RNG lunes.

$$\begin{cases} d(p_k, Q) < d(Q, p_j) - (2r_Q + r_j) & (13a) \\ d(p_k, p_j) < d(Q, p_j) - (r_Q + 2r_j), & (13b) \end{cases}$$

which are Equations 12 and thus holds by assumption. The consequence of the theorem is then $\max(d(p_k, x_i), d(p_k, x_j)) < d(x_i, x_j)$, for any x_i and x_j in the pivot domains of Q and p_j , respectively. Since the only member of the pivot Q is Q , then $\max(d(p_k, Q), d(p_k, x_j)) < d(Q, x_j)$. \square

Note that since Q is not really a pivot, we cannot simply lookup *GRNG* neighbors of it. Rather, Equations 12 must be explicitly checked for all pivots p_i that survive the elimination round of Stage I. Thus, additional entire pivot domains are eliminated, Figure 5.

Stage III: Pivot-Exemplar Interaction: This stage is symmetric with Stage II by enlarging the G-lune, but instead of using Q as a virtual pivot, an exemplar is used as a virtual, zero-radius pivot. These exemplar are constituents x_j of surviving pivots p_j .

Proposition 2. *If a pivot p_k falls in the G-lune of a parent (p_i, r_i) of Q and $(x_j, r_j = 0)$, i.e.,*

$$\begin{cases} d(p_k, p_i) < d(p_i, x_j) - 2r_i & (14a) \\ d(p_k, x_j) < d(p_i, x_j) - r_i, & (14b) \end{cases}$$

then $\max(d(p_k, Q), d(p_k, x_j)) < d(Q, x_j)$ and Q cannot have a *RNG* link with x_j .

Proof. Apply Theorem 1 with x_j as p_j with radii $r_j = 0$. Then, the condition of Theorem 1 is

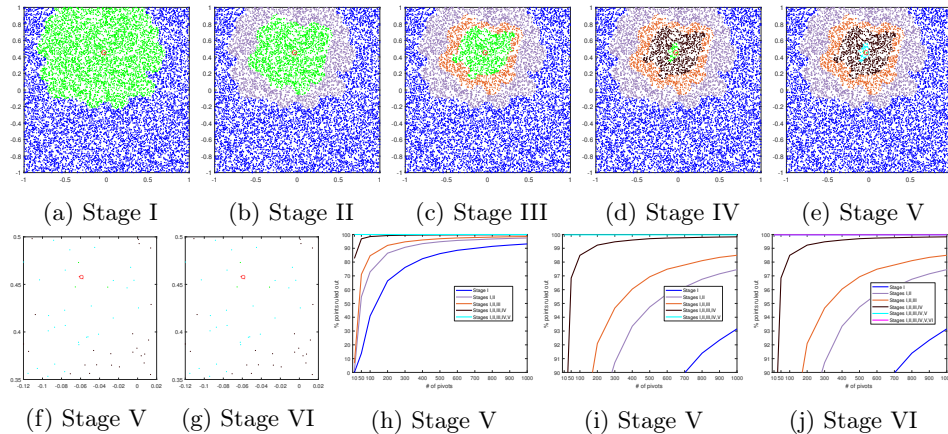


Fig. 5: The savings achieved by Stages I-VI for a GRNG-RNG Hierarchy with $M = 200$ pivots on a dataset of $N = 10,000$ uniformly distributed points in $[-1, 1]^2$ where the green area shows remaining exemplars after each stage. (f),(g),(i), and (j) are zoomed in.

$$\begin{cases} d(p_k, p_i) < d(p_i, x_j) - (2r_i + 0) & (15a) \\ d(p_k, x_j) < d(p_i, x_j) - (r_i + 0), & (15b) \end{cases}$$

which is the premise of the proposition. Then by Theorem 1, using Q as an exemplar in the pivot domain of p_i , and x_j as the sole exemplar in the pivot domain of x_j gives $\max(d(p_k, Q), d(p_k, x_j)) < d(Q, x_j)$. \square

In Stage III, then, for all parents of Q , (p_i, r_i) , and each exemplar x_j of the remaining pivots p_j , Equations 14 are checked which if valid rule out the exemplar x_j . Note that once a p_k is found that eliminates x_j , the process stops, so it is judicious to pick p_k in order of distance to p_i as closer pivots are more likely to fall in the G-lune of p_i and x_j , Figure 5.

Stage IV: Pivot-Mediated Exemplar-Exemplar Interactions: The aim of the next three stages is to prevent brute-force examination of all exemplars x_k potentially invalidating RNG link(Q, x_i) by falling in lune(Q, x_i). In Stage IV only pivots are checked, *i.e.*, whether pivot p_k satisfies

$$\max(d(p_k, Q), d(p_k, x_i)) < d(Q, x_i), \quad k = 1, 2, \dots, M. \quad (16)$$

Observe that only p_k for which $d(p_k, Q) < d(Q, x_i)$ need to be considered, and for those $d(p_k, x_i) < d(Q, x_i)$ is checked. Note that if one p_k satisfies this, link(Q, x_j) is invalidated and the process is stopped, Figure 5.

Stage V: Exemplar-Mediated Exemplar-Exemplar Interactions: In this stage, all the exemplars x_k which may invalidate the potential RNG link between Q and x_i are explored by checking

$$\max(d(Q, x_k), d(x_i, x_k)) < d(Q, x_i). \quad (17)$$

Observe that since the process stops if one x_k falls in the lune, so it is judicious to begin with a select group of x_k that would more likely fall in the lune(Q, x_i). First, the closest neighbors of x_i can be found by consulting the RNG neighbors of x_i and neighbors of neighbors, and so on until $d(x_i, x_k)$ exceeds $d(Q, x_i)$. Second, since some distances $d(Q, x_k)$ have been computed and cached for other purposes, these can be rank-ordered and these x_k can be explored until $d(Q, x_k)$ exceeds $d(Q, x_j)$, Figure 5.

Stage VI: RNG Link Verification: If the potential RNG link(Q, x_i) is not invalidated by the select group of exemplars x_k , the entire remaining set of x_k must exhaustively be considered to complete the verification. Note, however, that exemplars x_k in pivot domain p_k can be excluded from this consideration and without the costly computation of $d(Q, x_k)$ if the entire pivot domain is fully outside the lune(Q, x_i):

Proposition 3. *No exemplar x_k of pivot domain p_k can fall in lune(Q, x_i) if*

$$\max(d(Q, p_k) - \delta_{\max}(p_k), d(x_i, p_k) - \delta_{\max}(p_k)) \geq d(Q, x_i), \quad (18)$$

where $\delta_{\max}(p_k) = \max_{x_k, d(x_k, p_k) \leq r_k} d(p_k, x_k)$ is the maximum distance of exemplar $x_k \in \mathcal{D}(p_k, r_k)$ from p_k .

Proof. Let x_k be in the pivot domain of p_k . Then

$$\begin{cases} d(Q, x_k) \geq d(Q, p_k) - d(p_k, x_k) \geq d(Q, p_k) - \max_{\forall x_k, d(x_k, p_k) \leq r_k} d(p_k, x_k) \geq d(Q, x_j) & (19a) \\ d(x_j, x_k) \geq d(x_j, p_k) - d(p_k, x_k) \geq d(x_j, p_k) - \max_{\forall x_k, d(x_k, p_k) \leq r_k} d(p_k, x_k) \geq d(Q, x_j), & (19b) \end{cases}$$

or $\max(d(Q, x_k), d(x_j, x_k)) \geq d(Q, x_j)$, which puts x_k outside the lune(Q, x_j). \square

For the remaining pivot domains, the computation of $d(Q, x_k)$ can still be avoided for some exemplar x_k :

Proposition 4. Any exemplar x_k in the pivot domain of p_k for which

$$\max(d(Q, p_k) - d(x_k, p_k), d(x_i, p_k) - d(x_k, p_k)) \geq d(Q, x_i) \quad (20)$$

falls outside lune(Q, x_i).

Proof.

$$\begin{cases} d(Q, x_k) \geq d(Q, p_k) - d(x_k, p_k) \geq d(Q, x_j) & (21a) \\ d(x_j, x_k) \geq d(x_j, p_k) - d(x_k, p_k) \geq d(Q, x_j), & (21b) \end{cases}$$

or $\max(d(Q, x_k), d(x_j, x_k)) \geq d(Q, x_j)$, which puts x_k outside the lune(Q, x_j). \square

Any exemplar x_k which is not ruled out by Proposition 3 and 4 must now be explicitly considered. If none are in the lune(Q, x_i), then link(Q, x_i) is validated.

Stage VII: Existing RNG Link Validation: The above six stages locate Q in the RNG and identify its RNG neighbors. This is sufficient for a RNG search query. However, if the dataset \mathcal{S} is to be augmented with Q , a final check must be made as to which existing RNG links would be removed by the presence of Q . While this is a brute force $O(\alpha N)$ operation, it is important to avoid computing $d(Q, x_i)$ for all $x_i \in \mathcal{S}$. Observe that Q does not threaten links that are "too far" from it. This notion can be implemented if two parameters are maintained, one for exemplars and one for pivots:

$$\bar{\mu}_{\max}(x_i) = \max_{x_j \in \text{RNG}(x_i)} d(x_i, x_j), \mu_{\max}(p_i) = \max_{d(x_i, p_i) \leq r_i} [\bar{\mu}_{\max}(x_i) + d(x_i, p_i)]. \quad (22)$$

Proposition 5. A query Q does not invalidate RNG links at x_i if $d(Q, x_i) \geq \bar{\mu}_{\max}(x_i)$. A query Q does not invalidate any RNG link of any exemplars $x_i \in \mathcal{D}(p_i, r_i)$, if $d(Q, p_i) > \mu_{\max}(p_i)$.

Proof. The query Q lies outside lune(x_i, x_j) because

$$\max(d(Q, x_i), d(Q, x_j)) \geq d(Q, x_i) \geq \bar{\mu}_{\max}(x_i) \geq d(x_i, x_j). \quad (23)$$

Consider an arbitrary exemplar x_i in the pivot domain of p_i and show that $d(Q, x_i) \geq \bar{\mu}_{\max}(x_i)$ so:

$$d(Q, x_i) \geq d(Q, p_i) - d(p_i, x_i) \geq \mu_{\max}(p_i) - d(p_i, x_i) \geq \bar{\mu}_{\max}(x_i) + d(x_i, p_i) - d(p_i, x_i) \geq \bar{\mu}_{\max}(x_i). \quad (24)$$

\square

Algorithm 1: RNG Localization for Query Q in GRNG-RNG Hierarchy.

Input: Query Q , pivots \mathcal{P} , radius r_i for $p_i \in \mathcal{P}$, GRNG(\mathcal{P}), children $C(p_i)$ for $p_i \in \mathcal{P}$, max child distance $\delta_{\max}(p_i)$ for $p_i \in \mathcal{P}$, exemplar \mathcal{X} , RNG(\mathcal{X}), parents $P(x_i)$ for $x_i \in \mathcal{X}$, GRNG neighbors GRNG(x_i) for $x_i \in \mathcal{X}$.

Output: RNG neighbors of Q , Parents of Q , GRNG neighbors of Q .

- 1 **begin**
- 2 **Stage 1:** Find parents $P(Q) = \{p_i \in \mathcal{P} : d(Q, p_i) \leq r_i\}$. Collect potential GRNG neighbors of Q as $\mathcal{A}(\mathcal{P}) = \bigcup_{p_i \in P(Q)} \text{GRNG}(p_i)$. If $|P(Q)| = 0$, $\mathcal{A}(\mathcal{P}) = \mathcal{P}$.
- 3 **Stage 2:** Find GRNG(Q) by validating all potential neighbors $p_j \in \mathcal{A}(\mathcal{P})$. If no $p_k \in \mathcal{P}$ satisfies both $d(Q, p_k) < d(Q, p_j) - r_j$ and $d(p_j, p_k) < d(Q, p_j) - 2r_j$, then p_j is added to GRNG(Q).
- 4 **Stage 3:** Collect potential RNG neighbors of Q as $\mathcal{A}(\mathcal{X}) = \bigcup_{p_i \in P(Q)} C(p_i)$. Remove $x_j \in \mathcal{A}(\mathcal{X})$ if any $p_j \in P(x_j)$ is not in GRNG(Q). Remove $x_j \in \mathcal{A}(\mathcal{X})$ if any $p_i \in P(Q)$ is not in GRNG(x_j).
- 5 **Stage 4:** Consider invalidation of link(Q, x_j) for $x_j \in \mathcal{A}(\mathcal{X})$ by checking $p_k \in \text{GRNG}(Q)$ for interference. If any p_k satisfies both $d(Q, p_k) < d(Q, x_j)$ and $d(x_j, p_k) < d(Q, x_j)$, then x_j is removed from $\mathcal{A}(\mathcal{X})$.
- 6 **Stage 5:** Consider invalidation of link(Q, x_j) for $x_j \in \mathcal{A}(\mathcal{X})$ by checking $x_k \in \mathcal{A}(\mathcal{X})$ for interference. If any x_k satisfies both $d(Q, x_k) < d(Q, x_j)$ and $d(x_j, x_k) < d(Q, x_j)$, then x_j is removed from $\mathcal{A}(\mathcal{X})$.
- 7 **Stage 6:** Consider invalidation of link(Q, x_j) for $x_j \in \mathcal{A}(\mathcal{X})$ by performing exhaustive check for interference. Use $\delta_{\max}(p_k)$ and $C(p_k)$ for $p_k \in \mathcal{P}$ with Propositions 3 and 4 to narrow down the set of potentially interfering points x_k . If no x_k satisfies both $d(Q, x_k) < d(Q, x_j)$ and $d(x_j, x_k) < d(Q, x_j)$, then x_j is added to RNG(Q).
- 8 **end**

This proposition suggests a three-step procedure: (i) remove entire pivot domains if $d(Q, p_i) \geq \mu_{\max}(p_i)$; (ii) remove all exemplars in the remaining pivot domains for which $d(Q, x_i) \geq \bar{\mu}_{\max}(x_i)$; (iii) check the RNG condition explicitly for the remaining x_i and any x_j it links to. This completes the incremental update of \mathcal{S} to $\mathcal{S} \cup \{Q\}$.

Experimental Results The improvements due to this two-layer GRNG-RNG configuration are examined in experiments by varying dimensions and number of exemplars. Figure 6 examines the number of distance computations required for construction and search per stage as a function of the number of pivots. Observe that the first stage cost increases exponentially while the remaining stages experience an exponential drop. This is also observed for search distances per query. The total cost thus has an optimum for each. Since construction is offline while search is online, the number of pivots is optimized for the latter. Figure 6(c) examines the search costs for different dimensions. It is clear that search time rises exponentially with increasing dimension. Observe from Figure 6(b) that additional pivots would have enjoyed the exponential drop in all stages except for Stage I which involves GRNG Construction. If the cost of this stage as a function of M can be lowered, the overall cost will be decreased dramatically. The next section proposes a two-layer

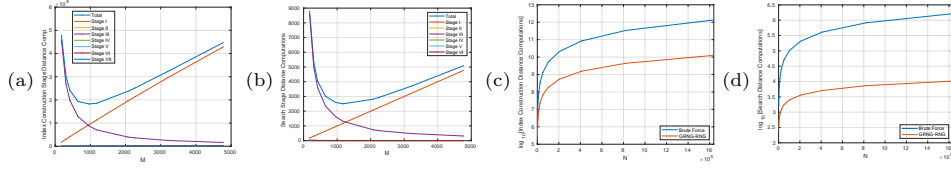


Fig. 6: Stage-by-stage distance computations for construction (a) and search (b) across different numbers of pivots M for $N=102,400$ exemplars uniformly distributed in 2D. Comparison of our GRNG-RNG hierarchy for RNG construction (c) and search (d) to a Brute Force RNG algorithm that precomputes all distances.

scheme for constructing GRNG using a coarser GRNG in the same way the RNG construction was guided by a GRNG.

3 Incremental Construction of the GRNG

The question naturally arises whether the construction of the GRNG of the pivot layer itself can benefit from a two-layer pivot-based indexing approach similar to the construction of the same for the RNG of the exemplars. Formally, let $\bar{\mathcal{P}} = \{(\bar{p}_i, \bar{r}_i) | i = 1, 2, \dots, \bar{M}\}$ denote pivots obtained from the previous section; refer to these as *fine-scale pivots* to distinguish them from the *coarse-scale pivots* $\mathcal{P} = \{(P_i, r_i) | i = 1, 2, \dots, M\}$. The idea is for each coarse-scale pivot p_i to represent a number of fine-scale pivots \bar{p}_i . Define the *Relative Pivot Domain* $\mathcal{D}(p_i, r_i)$ as the set of all fine-scale domain pivots (\bar{p}_i, \bar{r}_i) whose entire exemplar domain is within a radius of r_i , *i.e.*, $d(p_i, \bar{p}_i) \leq r_i - \bar{r}_i$. In this scenario, a query Q is either a fine-scale pivot for now with r_Q matching that of other fine-scale pivots, or it can be considered a fine-scale pivot with zero radius. The query computes $d(Q, p_i), i = 1, 2, \dots, M$ and if $d(Q, p_i) < r_i - r_Q$, p_i is a parent of Q . The question then arises as to what kind of graph structure for the coarse-scale pivots can efficiently locate a query in the GRNG of the fine-scale pivots. The following shows that the GRNG of coarse-scale pivots can accomplish this:

Stage I: “Coarse-Scale Pivot” - “Coarse-Scale Pivot” Interactions:

Theorem 2. Consider two fine-scale pivots $(\bar{p}_i, \bar{r}_i) \in \mathcal{D}(p_i, r_i)$ and $(\bar{p}_j, \bar{r}_j) \in \mathcal{D}(p_j, r_j)$. Then, if (p_i, r_i) and (p_j, r_j) do not share a GRNG link, (\bar{p}_i, \bar{r}_i) and (\bar{p}_j, \bar{r}_j) cannot have a GRNG link either.

Proof. Since \bar{p}_i and \bar{p}_j are in the relative-pivot domain of their coarse-scale pivots p_i and p_j , respectively,

$$\begin{cases} d(\bar{p}_i, p_i) \leq r_i - \bar{r}_i & (25a) \\ d(\bar{p}_j, p_j) \leq r_j - \bar{r}_j. & (25b) \end{cases}$$

That p_i and p_j do not have a GRNG link implies that there exists a coarse-level pivot p_k such that

$$\begin{cases} d(p_k, p_i) < d(p_i, p_j) - (2r_i + r_j) & (26a) \\ d(p_k, p_j) < d(p_i, p_j) - (r_i + 2r_j), & (26b) \end{cases}$$

i.e., p_k is in the G-lune of p_i and p_j . It is now shown that p_k is also in the G-lune of fine-scale pivots \bar{p}_i and \bar{p}_j , and since all coarse-scale pivots are also fine-scale pivots, a GRNG link does not exist between \bar{p}_i and \bar{p}_j .

Observe first that $d(p_k, \bar{p}_i)$ can be related to $d(p_k, p_i)$ by a double application of the triangle inequality, and similarly for the $d(p_k, \bar{p}_j)$,

$$\begin{cases} d(p_k, \bar{p}_i) \leq d(p_k, p_i) + d(p_i, \bar{p}_i) \leq d(p_k, p_i) + (r_i - \bar{r}_i) < d(p_i, p_j) - (2r_i + r_j) + (r_i - \bar{r}_i) = d(p_i, p_j) - r_i - r_j - \bar{r}_i & (27a) \\ d(p_k, \bar{p}_j) \leq d(p_k, p_j) + d(p_j, \bar{p}_j) \leq d(p_k, p_j) + (r_j - \bar{r}_j) < d(p_i, p_j) - (r_i + 2r_j) + (r_j - \bar{r}_j) = d(p_i, p_j) - r_i - r_j - \bar{r}_j. & (27b) \end{cases}$$

Similarly, $d(p_i, p_j)$ can be related to $d(\bar{p}_i, \bar{p}_j)$ by an application of the triangle inequality

$$d(p_i, p_j) \leq d(p_i, \bar{p}_i) + d(\bar{p}_i, \bar{p}_j) + d(\bar{p}_j, p_j) \leq d(\bar{p}_i, \bar{p}_j) + (r_i - \bar{r}_i) + (r_j - \bar{r}_j). \quad (28)$$

Combining Equations 27 and 28

$$\begin{cases} d(p_k, \bar{p}_i) < d(\bar{p}_i, \bar{p}_j) + (r_i - \bar{r}_i) + (r_j - \bar{r}_j) - r_i - r_j - \bar{r}_i = d(\bar{p}_i, \bar{p}_j) - (2\bar{r}_i + \bar{r}_j) & (29a) \\ d(p_k, \bar{p}_j) < d(\bar{p}_i, \bar{p}_j) + (r_i - \bar{r}_i) + (r_j - \bar{r}_j) - r_i - r_j - \bar{r}_j = d(\bar{p}_i, \bar{p}_j) - (\bar{r}_i + 2\bar{r}_j), & (29b) \end{cases}$$

showing that p_k falls in the G-lune of $d(\bar{p}_i, \bar{p}_j)$ and thus no GRNG link can exist between them. \square

This theorem, in analogy to Theorem 1 of the previous section, allows for the efficient localization of a query Q for search in stating that the fine-scale GRNG neighbors of Q are only among children of coarse-scale GRNG neighbors of Q 's parents, thus, removing entire pivot domains of non-neighbors, see Figure 7.

Stage II: Query - ‘‘Coarse-Scale Pivot’’ Interactions: In this stage, (Q, r_Q) is considered as a virtual pivot.

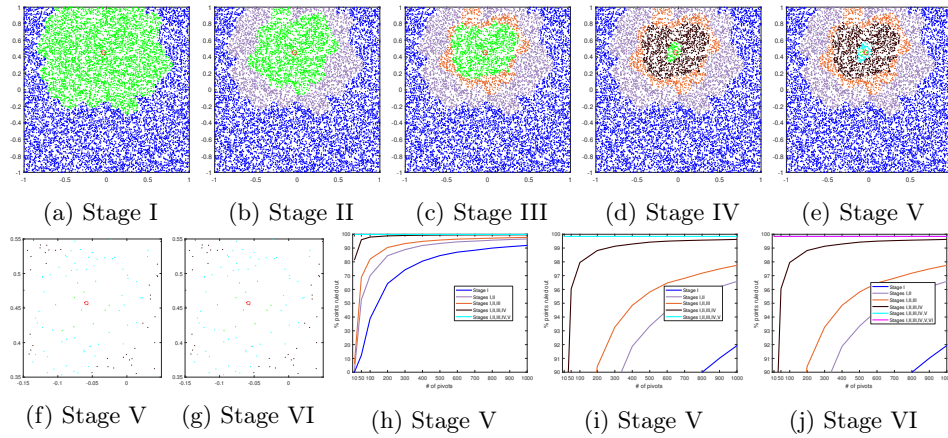


Fig. 7: The savings achieved by Stages I-VI for a GRNG-GRNG Hierarchy of $M = 200$ pivots with radius $r = 0.005$ on a dataset of 10,000 uniformly distributed points in $[-1, 1]^2$ where the green area shows remaining exemplars after each stage. (f),(g),(i), and (j) are zoomed in.

Proposition 6. *The query Q does not form GRNG links with any children (\bar{p}_i, \bar{r}_i) of those coarse-scale pivots (p_i, r_i) that do not form a GRNG link with Q when considered as a virtual pivot with $r_Q = 0$.*

Proof. Apply Theorem 2 with (Q, \bar{r}_Q) acting both as (p_i, r_i) and also as (\bar{p}_i, \bar{r}_i) , i.e., Q is a coarse-scale pivot with a single member, itself, since $r_i - \bar{r}_i = \bar{r}_Q - \bar{r}_Q = 0$. \square

Stage III: “Coarse-Scale Pivot” – “Fine-Scale Pivot” Interactions: This stage is mirror symmetric to Stage II, except that instead of treating Q as a virtual coarse-scale pivot, a specific fine-scale pivot (\bar{p}_j, \bar{r}_j) is considered a virtual pivot.

Proposition 7. *If (\bar{p}_j, \bar{r}_j) does not form a coarse-scale GRNG link with a parent (p_i, r_i) of Q , then (\bar{p}_j, \bar{r}_j) does not form a fine-scale GRNG link with (Q, r_Q) .*

The proof is simply an application of Theorem (2) with (\bar{p}_j, \bar{r}_j) considered as both a fine-scale and a coarse-scale pivot. This third stage rules out all the remaining fine-scale pivots which are not a GRNG neighbor of **all** Q ’s parents, Figure 7.

Stage IV: “Coarse-Scale Pivot”–Mediated “Fine-Scale Pivot” Interactions: All the GRNG links between the remaining fine-scale pivots and Q must now be investigated. In Stage IV only coarse-scale pivots are considered as potential occupiers of the G-lune by probing

$$\begin{cases} d(p_k, Q) < d(Q, \bar{p}_j) - (2\bar{r}_Q + \bar{r}_j) & (30a) \\ d(p_k, \bar{p}_j) < d(Q, \bar{p}_j) - (\bar{r}_Q + 2\bar{r}_j). & (30b) \end{cases}$$

Since $d(Q, \bar{p}_j) - (2\bar{r}_Q + \bar{r}_j)$ is a known value, only pivots p_k closer to Q than this value need to be considered. Similarly, for $d(\bar{p}_j, \bar{r}_j) \in \mathcal{D}(p_j, r_j)$, observe that $d(p_k, \bar{p}_j) \geq d(p_k, p_j) - (r_j - \bar{r}_j)$, so that if $d(p_k, p_j) \geq d(Q, \bar{p}_j) - (r_Q + 2\bar{r}_j) + (r_j - \bar{r}_j)$, then Equation (30b) does not hold and there is no need to consider such p_k . Thus, very few p_k are actually considered, Figure 7.

Stage V: “Fine-Scale Pivot” – Mediated “Fine-Scale Pivot” Interactions: Those links between Q and \bar{p}_j that survive the pivot test must now test against occupancy of G-lune(Q, \bar{p}_j) by exemplars \bar{p}_k . In this stage, a select group of \bar{p}_k , namely those close to Q and \bar{p}_j which are more likely to be in G-lune(Q, \bar{p}_j) are considered, leaving the rest to Stage VI. Specifically, these are the $k = 25$ nearest neighbors of Q and \bar{p}_j , Figure 7.

Stage VI: “Fine-Scale Pivot” “Fine-Scale Pivot” Interactions: Very few fine-scale pivots \bar{p}_j remain at this stage. These need to be validated with all other fine-scale pivots \bar{p}_k . However, the following proposition prevents consideration of a majority of them. Define

$$\delta_{\max}(p_k) = \max_{\forall \bar{p}_k, d(p_k, \bar{p}_k) \leq (r_k - \bar{r}_k)} d(p_k, \bar{p}_k). \quad (31)$$

Proposition 8. *All fine-scale pivots $(\bar{p}_k, \bar{r}_k) \in \mathcal{D}(p_k, r_k)$ satisfying*

$$\begin{cases} d(Q, p_k) - \delta_{\max}(p_k) \geq d(Q, \bar{p}_j) - (2\bar{r}_Q + \bar{r}_j) & (32a) \\ d(\bar{p}_j, p_k) - \delta_{\max}(p_k) \geq d(Q, \bar{p}_j) - (2\bar{r}_j + \bar{r}_Q) & (32b) \end{cases}$$

fall outside the G-lune(Q, \bar{p}_j), for a query (Q, \bar{r}_Q) and a fine-scale pivot (\bar{p}_j, \bar{r}_j) .

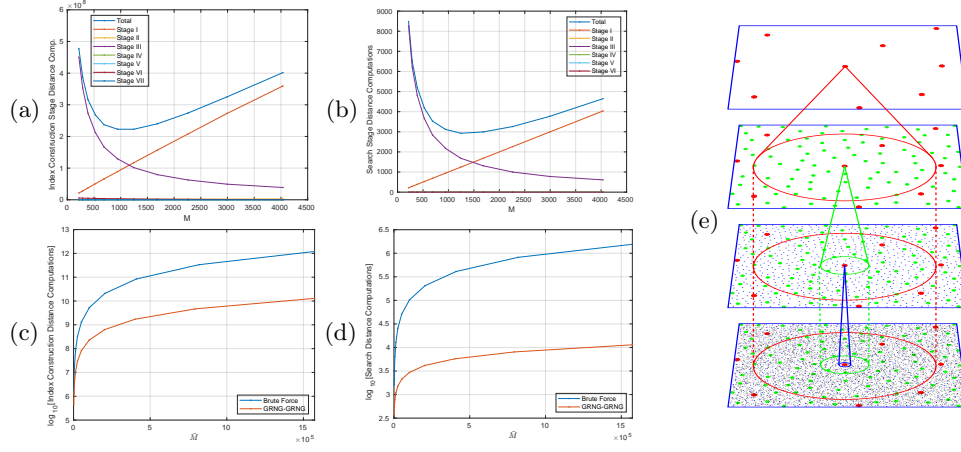


Fig. 8: Stage by stage analysis for GRNG-GRNG hierarchy for $\bar{M} = 102,400$ uniformly distributed fine-scale pivots in 2D as a function of M , the number of coarse-scale pivots. The number of distance computations for construction (a) and search (b) show Stage I is increasing with M while other stages exponentially decay with an optimum for each in total. The improvements of GRNG-GRNG with respect to brute-force as a function of M for construction (c) and search (d) distances is significant. (e) The monotonically increasing Stage I in (a-b) suggest using a multi-layer hierarchy.

Proof. Observe that

$$\begin{cases} d(Q, \bar{p}_k) \geq d(Q, p_k) - d(\bar{p}_k, p_k) \geq d(Q, p_k) - \max_{\forall \bar{p}_k, d(p_k, \bar{p}_k) \leq (r_k - \bar{r}_k)} d(\bar{p}_k, p_k) = d(Q, p_k) - \delta_{\max}(p_k), & (33a) \\ d(\bar{p}_j, \bar{p}_k) \geq d(\bar{p}_j, p_k) - d(\bar{p}_k, p_k) \geq d(\bar{p}_j, p_k) - \max_{\forall \bar{p}_k, d(p_k, \bar{p}_k) \leq (r_k - \bar{r}_k)} d(\bar{p}_k, p_k) = d(\bar{p}_j, p_k) - \delta_{\max}(p_k). & (33b) \end{cases}$$

Now, combining Equations 32 and 33,

$$\begin{cases} d(Q, \bar{p}_k) \geq d(Q, \bar{p}_j) - (2\bar{r}_Q + \bar{r}_j) & (34a) \\ d(\bar{p}_j, \bar{p}_k) \geq d(Q, \bar{p}_j) - (\bar{r}_Q + 2\bar{r}_j), & (34b) \end{cases}$$

i.e., \bar{p}_k cannot be inside the G-lune(Q, \bar{p}_j). \square

This proposition excludes entire pivot domains from the validation process. The following proposition further restricts the remaining sets.

Proposition 9. All fine-scale pivots $(\bar{p}_k, \bar{r}_k) \in \mathcal{D}(p_k, r_k)$ satisfying

$$\begin{cases} d(Q, p_k) - d(p_k, \bar{p}_k) \geq d(Q, \bar{p}_j) - (2\bar{r}_Q + \bar{r}_j) & (35a) \\ d(\bar{p}_j, p_k) - d(p_k, \bar{p}_k) \geq d(Q, \bar{p}_j) - (\bar{r}_Q + 2\bar{r}_j), & (35b) \end{cases}$$

falls outside the GRNG-lune(Q, \bar{p}_j) for a query (Q, \bar{r}_Q) and a fine-scale pivot (\bar{p}_j, \bar{r}_j).

Proof. Combine the first inequality in Equations 33 with the premise to show Equations 35. \square

After the majority of fine-scale pivots (\bar{p}_k, \bar{r}_k) have been eliminated, the remaining ones must test the two GRNG conditions. For efficiency, if first condition $d(Q, \bar{p}_k) < d(Q, \bar{p}_j - (2\bar{r}_Q + \bar{r}_j))$ does not hold, the second condition $d(\bar{p}_j, \bar{p}_k) < d(Q, \bar{p}_j - (\bar{r}_Q + 2\bar{r}_j))$ need not be tested, Figure 7.

Stage VII: “Coarse-Scale Pivot” – “Fine-Scale Pivot” Validations: The incremental construction requires checking which existing GRNG links may be invalidated by the addition of Q . Define first,

$$\begin{cases} \bar{\mu}_{\max}(\bar{p}_i) = \max_{\bar{p}_j, \text{GRNG}(\bar{p}_i)} [d(\bar{p}_i, \bar{p}_j) - (2\bar{r}_i + \bar{r}_j)] \\ \mu_{\max}(p_i) = \max_{\forall(\bar{p}_i, \bar{r}_i) \in \mathcal{D}(p_i, r_i)} [\bar{\mu}_{\max}(\bar{p}_i) + d(p_i, \bar{p}_i)]. \end{cases} \quad (36a)$$

$$\quad (36b)$$

Proposition 10. *The insertion of Q does not invalidate any GRNG links involving fine-scale pivot \bar{p}_i for which*

$$d(Q, \bar{p}_i) \geq \bar{\mu}_{\max}(\bar{p}_i). \quad (37)$$

Furthermore, the insertion of Q does not interfere with the GRNG link involving fine-scale pivots $(\bar{p}_i, \bar{r}_i) \in \mathcal{D}(p_i, r_i)$ if

$$d(Q, p_i) \geq \mu_{\max}(p_i). \quad (38)$$

Proof. It is clear that if $d(Q, \bar{p}_i) \geq \bar{\mu}_{\max}(\bar{p}_i)$, then $\forall \bar{p}_j$

$$d(Q, \bar{p}_i) \geq d(\bar{p}_i, \bar{p}_j) - (2\bar{r}_i + \bar{r}_j), \quad (39)$$

so that Q is outside G-lune (\bar{p}_i, \bar{p}_j) . By the triangle inequality,

$$\begin{aligned} d(Q, \bar{p}_i) &\geq d(Q, p_i) - d(p_i, \bar{p}_i) \\ &\geq \mu_{\max}(p_i) - d(p_i, \bar{p}_i) \\ &\geq \max_{\forall \bar{p}_k, d(p_i, \bar{p}_k) \leq r_i - \bar{r}_k} (\bar{\mu}_{\max}(\bar{p}_k) + d(p_i, \bar{p}_k)) - d(p_i, \bar{p}_i) \\ &\geq \bar{\mu}_{\max}(\bar{p}_i) + d(p_i, \bar{p}_i) - d(p_i, \bar{p}_i) \\ &\geq \bar{\mu}_{\max}(\bar{p}_i). \end{aligned} \quad (40)$$

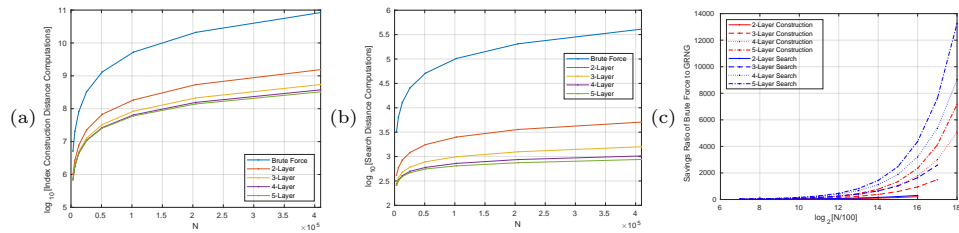


Fig. 9: Comparing the efficiency of multi-layer GRNG hierarchies on 2D uniformly distributed data to a Brute Force algorithm that would precompute all pairwise distances (a) for RNG construction or precompute all N distances to dataset members (b) for search. (c) The ratio of distance computation savings across N and number of layers.

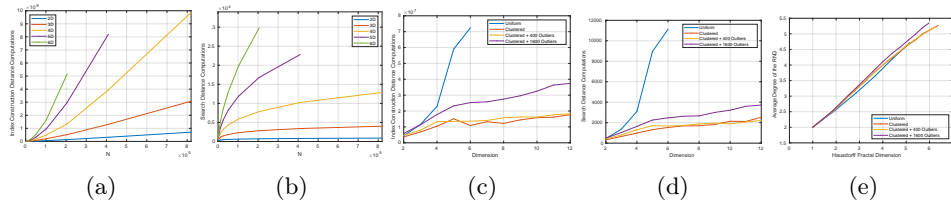


Fig. 10: The distance computations for index construction (a) and search (b) increases as a function of number of exemplars and dimensions. However, with clustered data (c)(d), even with outliers, both construction costs and search distances increase much less rapidly. (e) The average degree of the RNG is related to the intrinsic dimensionality.

Thus, Q cannot interfere with any GRNG link formed from \bar{p}_i . □

The proposition suggests a three-step approach to examining existing links: (i) Remove all coarse-scale pivot domains p_i satisfying Equation 38; (ii) Remove all fine-scale pivot domains (\bar{p}_i, \bar{r}_i) satisfying Equation 37; (iii) For any remaining fine-scale pivot (\bar{p}_i, \bar{r}_i) connecting with (\bar{p}_j, \bar{r}_j) , if Q is in the G -lune (\bar{p}_i, \bar{p}_j) , then the link needs to be removed.

4 Experiments

Experiments on uniformly distributed and clustered synthetic data in \mathcal{R}^d show the effectiveness of the proposed approach. Note that for all datasets where brute-force is possible, the RNG has been validated for exactness. Figure 9(a) shows that our method is effective in uniformly distributed data and a hierarchy helps, although the optimal number of layers depends on N . Figure 9(b) shows that search is extremely efficient and is essentially logarithmic in N . Figure 10 shows that construction costs are exponential in N and dimension d for uniform data (but search remains logarithmic), in contrast to clustered data where both construction and search costs are well-behaved, Figure 10(c,d). Figure 10(e) shows that the connectivity of RNG is effectively linear in intrinsic dimension of the data.

Experiments on several real-world datasets, namely, COREL, MNIST, and LA. For MNIST, a neural network trained using triplet loss was used to reduce the 784D Euclidean representation into 64D. The results are shown in Table 4. These results show that our method is significantly more efficient while also producing the exact RNG.

References

1. Chavez, E., Dobrev, S., Kranakis, E., Opatrny, J., Stacho, L., Tejada, H., Urrutia, J.: Half-space proximal: A new local test for extracting a bounded dilation spanner of a unit disk graph. In: International Conference On Principles Of Distributed Systems. pp. 235–245. Springer (2005)
2. Chávez, E., Navarro, G., Baeza-Yates, R., Marroquín, J.L.: Searching in metric spaces. ACM computing surveys (CSUR) **33**(3), 273–321 (2001)
3. Delaunay, B.: Sur la sphère vide. A la mémoire de Georges Voronoï. Bulletin de l’Académie des Sciences de l’URSS pp. 793–800 (1934)

Table 1: Statistics for Optimal 2-Layer GRNG-RNG Hierarchies on Uniformly Distributed Data.

Search Distance Computations						Search Time (ms)					
N	2D	3D	4D	5D	6D	N	2D	3D	4D	5D	6D
1,600	281.77	463.03	696.97	950.93	1,196.06	1,600	0.274	0.427	0.978	2.080	3.649
3,200	414.40	701.99	1,089.12	1,552.94	2,055.56	3,200	0.400	0.723	2.300	4.752	5.987
6,400	594.15	1,042.35	1,614.03	2,452.24	3,379.85	6,400	0.653	1.314	3.506	8.705	19.454
12,800	846.60	1,511.29	2,453.67	3,773.75	5,454.52	12,800	0.867	1.974	4.250	15.986	42.176
25,600	1,213.10	2,187.77	3,634.22	5,677.06	8,489.30	25,600	1.477	3.334	7.012	25.474	77.990
51,200	1,757.14	3,136.99	5,348.49	8,603.36	13,014.10	51,200	1.644	5.190	12.655	47.144	124.103
102,400	2,508.88	4,527.96	7,808.32	12,859.70	20,154.40	102,400	3.375	6.682	17.684	67.754	226.059
204,800	3,591.85	6,601.45	11,373.70	18,972.20	30,015.00	204,800	5.638	8.909	28.389	91.606	290.796
409,600	5,083.95	9,388.31	16,636.20	28,045.50		409,600	6.304	12.289	30.600	118.376	
819,200	7,297.52	13,491.90	23,792.50	41,247.20		819,200	11.481	18.770	52.273	141.868	
1,638,400	10,331.30	19,432.80	34,413.90			1,638,400	14.739	30.528	53.540		

Index Construction Distance Computations						
N	$N(N-1)/2$	2D	3D	4D	5D	6D
1,600	1,279,200	323,362	576,421	871,615	1,265,981	1,424,701
3,200	5,118,400	998,165	1,746,168	2,980,553	4,380,391	5,389,184
6,400	20,476,800	2,731,860	5,268,490	9,124,159	13,977,441	20,194,814
12,800	81,913,600	7,756,808	15,056,026	27,667,618	46,749,155	69,953,472
25,600	327,667,200	22,781,408	42,295,510	76,583,845	141,335,210	234,636,962
51,200	1,310,694,400	67,708,441	121,429,407	225,220,284	417,456,903	723,257,748
102,400	5,242,828,800	184,344,339	346,602,393	644,199,988	1,205,946,173	2,193,952,436
204,800	20,971,417,600	540,102,922	982,784,171	1,804,674,193	3,399,421,853	6,398,877,358
409,600	83,885,875,200	1,543,057,134	2,792,989,300	5,108,689,230	9,550,546,084	
819,200	335,543,910,400	4,381,197,495	7,939,742,585	14,528,254,634	26,692,822,584	
1,638,400	1,342,176,460,800	12,537,531,662	22,602,120,265	41,198,331,167		

Index Construction Time (hr)					
N	2D	3D	4D	5D	6D
1,600	3.931E-03	1.906E-04	6.376E-04	1.665E-03	7.062E-03
3,200	3.707E-04	6.220E-04	2.416E-03	6.863E-03	1.566E-02
6,400	1.336E-03	2.151E-03	7.185E-03	5.037E-02	9.357E-02
12,800	1.955E-03	6.007E-03	2.009E-02	0.104	0.353
25,600	5.727E-03	2.572E-02	5.196E-02	0.381	1.434
51,200	1.312E-02	0.242	0.228	1.214	4.176
102,400	4.814E-02	0.509	0.633	3.557	13.573
204,800	0.153	0.737	1.792	9.514	39.091
409,600	0.382	1.703	4.038	23.313	
819,200	1.718	3.139	11.183	54.078	
1,638,400	2.821	7.641	25.147		

Memory Usage (GB)					
N	2D	3D	4D	5D	6D
1,600	5.428E-03	6.954E-03	1.033E-02	1.785E-02	2.692E-02
3,200	8.476E-03	1.219E-02	2.136E-02	3.832E-02	6.510E-02
6,400	1.360E-02	2.262E-02	4.289E-02	7.547E-02	0.159
12,800	2.436E-02	4.267E-02	8.587E-02	0.174	0.345
25,600	4.607E-02	8.223E-02	0.179	0.401	0.862
51,200	8.268E-02	0.156	0.370	0.8815	1.981
102,400	0.157	0.312	0.778	1.949	4.587
204,800	0.317	0.625	1.602	4.161	10.251
409,600	0.633	1.258	3.299	8.947	
819,200	1.258	2.531	6.856	18.824	
1,638,400	2.531	5.181	14.194		

Table 2: Statistics for Optimal 3-Layer GRNG-GRNG-RNG Hierarchies on Uniformly Distributed Data.

Search Distance Computations						Search Time (ms)					
N	2D	3D	4D	5D	6D	N	2D	3D	4D	5D	6D
1,600	212.14	435.44	698.10	952.02	1,219.46	1,600	0.289	0.926	1.718	5.164	9.070
3,200	282.71	622.46	1,073.40	1,557.88	2,074.42	3,200	0.357	1.199	3.165	8.746	18.928
6,400	366.40	836.98	1,566.64	2,451.58	3,382.67	6,400	0.436	1.682	6.410	20.792	34.202
12,800	477.65	1,139.28	2,270.06	3,739.39	5,450.51	12,800	0.571	2.372	9.189	27.869	73.279
25,600	608.46	1,513.72	3,178.08	5,611.01	8,510.70	25,600	0.945	3.319	15.835	53.142	145.327
51,200	782.17	1,980.12	4,360.25	8,262.83	13,001.20	51,200	1.288	4.122	22.940	74.519	151.275
102,400	992.31	2,575.46	5,906.43	11,871.50	19,817.10	102,400	1.608	6.780	33.555	109.313	231.166
204,800	1,252.96	3,317.01	7,841.76	16,810.30	29,527.10	204,800	1.607	8.223	44.257	144.389	294.095
409,600	1,591.09	4,240.76	10,296.60	23,215.30	43,297.60	409,600	2.119	8.821	69.808	189.334	504.418
819,200	1,990.32	5,406.54	13,521.00	31,769.40		819,200	3.524	11.882	69.172	273.151	
1,638,400	2,514.94	6,927.56				1,638,400	2.865	11.776			
3,276,800	3,201.18	8,794.71				3,276,800	3.690	16.5714			
6,553,600	3,999.04	11,263.40				6,553,600	5.908	20.0029			
13,107,200	5,067.76					13,107,200	5.873				

Index Construction Distance Computations						
N	N(N-1)/2	2D	3D	4D	5D	6D
1,600	1,279,200	265,623	516,628	760,225	1,029,621	1,221,605
3,200	5,118,400	715,370	1,529,411	2,545,681	3,502,217	4,533,864
6,400	20,476,800	1,875,159	4,237,192	7,647,949	11,573,618	16,048,613
12,800	81,913,600	4,914,263	11,882,697	22,838,137	36,807,770	54,388,897
25,600	327,667,200	12,777,657	32,292,006	65,019,984	112,659,381	176,000,348
51,200	1,310,694,400	32,927,002	84,975,099	182,367,161	333,940,276	545,109,215
102,400	5,242,828,800	84,017,423	222,786,598	499,604,440	967,623,862	1,653,233,653
204,800	20,971,417,600	213,276,161	578,454,113	1,334,902,118	2,724,468,870	4,878,923,837
409,600	83,885,875,200	545,584,549	1,490,406,238	3,515,273,754	7,508,607,499	14,083,342,711
819,200	335,543,910,400	1,377,413,839	3,818,355,231	9,212,801,209	20,370,378,025	
1,638,400	1,342,176,460,800	3,497,518,219	9,781,461,413			
3,276,800	5,368,707,481,600	8,902,672,288	25,018,301,725			
6,553,600	21,474,833,203,200	22,597,217,032	64,078,700,856			
13,107,200	85,899,339,366,400	57,317,868,141				

Index Construction Time (hr)						Memory Usage (GB)					
N	2D	3D	4D	5D	6D	N	2D	3D	4D	5D	6D
1,600	1.370E-04	4.368E-04	8.014E-04	2.883E-03	4.154E-03	1,600	6.199E-03	8.556E-03	1.305E-02	2.096E-02	2.599E-02
3,200	3.161E-04	1.171E-03	2.966E-03	1.314E-02	1.711E-02	3,200	9.457E-03	1.443E-02	2.731E-02	4.394E-02	7.261E-02
6,400	7.230E-04	2.794E-03	1.024E-02	3.564E-02	6.159E-02	6,400	1.579E-02	2.674E-02	4.927E-02	9.863E-02	0.154
12,800	1.752E-03	7.762E-03	3.132E-02	9.312E-02	0.266	12,800	2.802E-02	4.917E-02	0.115	0.220	0.386
25,600	1.723E-02	2.074E-02	0.101	0.399	1.768	25,600	5.230E-02	0.101	0.238	0.481	0.928
51,200	1.508E-02	5.164E-02	0.296	0.928	2.158	51,200	9.154E-02	0.186	0.469	1.044	2.165
102,400	3.599E-02	0.164	0.868	2.607	8.542	102,400	0.177	0.365	0.966	2.299	5.000
204,800	6.814E-02	0.399	2.293	7.878	15.067	204,800	0.345	0.714	1.964	4.882	11.097
409,600	0.178	0.999	7.774	19.018	50.068	409,600	0.680	1.400	3.951	10.228	24.772
819,200	0.638	2.708	13.508	48.048		819,200	1.344	2.747	7.954	21.361	
1,638,400	1.074	4.365				1,638,400	2.940	5.678			
3,276,800	2.416	12.095				3,276,800	5.851	10.669			
6,553,600	8.062	26.993				6,553,600	11.665	22.260			
13,107,200	16.734					13,107,200	23.370				

Table 3: Statistics for Optimal GRNG Hierarchies on Uniformly Distributed Data.

Search Distance Computations						Search Time (ms)					
N	2D	3D	4D	5D	6D	N	2D	3D	4D	5D	6D
1,600	203.07	435.44	696.97	950.93	1,196.06	1,600	0.416	0.926	0.978	2.080	3.649
3,200	260.03	622.46	1,073.40	1,552.94	2,055.56	3,200	0.550	1.199	3.165	4.752	5.987
6,400	320.48	836.98	1,566.64	2,451.58	3,379.85	6,400	1.326	1.682	6.410	20.792	19.454
12,800	388.54	1,135.04	2,270.06	3,739.39	5,454.52	12,800	1.008	3.961	9.189	27.869	42.176
25,600	464.61	1,461.50	3,178.08	5,611.01	8,510.70	25,600	1.510	5.804	15.835	53.142	145.327
51,200	541.92	1,845.55	4,360.25	8,262.83	13,001.20	51,200	1.711	7.246	22.940	74.519	151.275
102,400	624.96	2,314.21	5,906.43	11,871.50	19,817.10	102,400	3.488	7.627	33.555	109.313	231.166
204,800	709.05	2,838.78	7,841.76	16,785.40	29,728.20	204,800	3.837	10.204	44.257	275.756	429.461
409,600	799.18	3,399.34	10,230.80	22,788.50		409,600	4.607	20.330	87.536	357.445	
819,200	888.07	4,009.96	12,870.40			819,200	4.155	17.256	106.133		
1,638,400	982.24	4,702.36	15,859.40			1,638,400	4.111	20.921	132.551		
3,276,800	1,072.47	5,457.28				3,276,800	5.026	20.941			
6,553,600	1,168.89	6,224.37				6,553,600	5.229	33.643			
13,107,200	1,264.24					13,107,200	6.217				
26,214,400	1,359.76					26,214,400	7.024				

Optimal Number of Layers, L						Index Construction Distance Computations						
N	2D	3D	4D	5D	6D	N	N(N-1)/2	2D	3D	4D	5D	6D
1,600	4	3	2	2	2	1,600	1,279,200	264,911	516,628	871,615	1,265,981	1,424,701
3,200	4	3	3	2	2	3,200	5,118,400	685,955	1,529,411	2,545,681	4,380,391	5,389,184
6,400	5	3	3	3	2	6,400	20,476,800	1,808,727	4,237,192	7,647,949	11,573,618	20,194,814
12,800	5	4	3	3	2	12,800	81,913,600	4,418,773	12,527,095	22,838,137	36,807,770	69,953,472
25,600	6	4	3	3	3	25,600	327,667,200	10,999,945	32,634,271	65,019,984	112,659,381	176,000,348
51,200	6	4	3	3	3	51,200	1,310,694,400	25,725,358	83,754,842	182,367,161	333,940,276	545,109,215
102,400	7	4	3	3	3	102,400	5,242,828,800	61,217,847	209,606,677	499,604,440	967,623,862	1,653,233,653
204,800	7	4	4	4	3	204,800	20,971,417,600	138,971,047	517,808,692	1,334,902,118	2,959,923,254	5,150,670,019
409,600	8	5	4	4		409,600	83,885,875,200	317,976,622	1,308,344,233	3,942,824,032	8,199,558,499	
819,200	8	5	4			819,200	335,543,910,400	707,049,296	3,074,992,726	9,863,795,760		
1,638,400	9	5	4			1,638,400	1,342,176,460,800	1,580,489,249	7,196,074,192	24,264,742,122		
3,276,800	9	5				3,276,800	5,368,707,481,600	3,451,125,580	16,680,031,216			
6,553,600	9	6				6,553,600	21,474,833,203,200	7,495,962,620	39,314,844,606			
13,107,200	10					13,107,200	85,899,339,366,400	16,340,695,641				
26,214,400	10					26,214,400	343,597,370,572,800	35,074,351,743				

Index Construction Time (hr)						Memory Usage (GB)					
N	2D	3D	4D	5D	6D	N	2D	3D	4D	5D	6D
1,600	2.306E-04	4.368E-04	6.376E-04	1.665E-03	7.062E-03	1,600	6.969E-03	8.556E-03	1.033E-02	1.785E-02	2.692E-02
3,200	5.619E-04	1.171E-03	2.966E-03	6.863E-03	1.566E-02	3,200	1.107E-02	1.443E-02	2.731E-02	3.832E-02	6.510E-02
6,400	3.079E-03	2.794E-03	1.024E-02	3.564E-02	9.357E-02	6,400	2.230E-02	2.674E-02	4.927E-02	9.863E-02	0.159
12,800	4.362E-03	1.594E-02	3.132E-02	9.312E-02	0.353	12,800	4.011E-02	6.742E-02	0.115	0.220	0.345
25,600	1.378E-02	5.056E-02	0.101	0.399	1.768	25,600	9.842E-02	0.121	0.238	0.481	0.928
51,200	3.004E-02	0.110	0.296	0.928	2.158	51,200	0.179	0.235	0.469	1.044	2.165
102,400	0.135	0.232	0.868	2.607	8.542	102,400	0.407	0.453	0.966	2.299	5.000
204,800	1.025	0.585	2.293	14.793	21.961	204,800	0.814	0.877	1.964	6.864	12.637
409,600	1.106	2.546	14.219	39.001		409,600	1.794	2.292	5.754	14.385	
819,200	2.664	3.936	23.547			819,200	3.476	4.420	11.410		
1,638,400	2.181	10.055	58.863			1,638,400	7.612	8.559	22.185		
3,276,800	21.782	21.594				3,276,800	14.775	16.697			
6,553,600	37.572	58.467				6,553,600	28.952	42.420			
13,107,200	48.889					13,107,200	67.396				
26,214,400	98.506					26,214,400	132.520				

Table 4: Results for real world datasets. (top) Corel, $N = 68,040$ in 57D, (middle) MNIST, $N = 60,000$ instances with 64D embeddings obtained through a neural network, and (bottom) LA, $N = 1,073,727$ instances in 2D. Accuracy is established by comparison to the brute-force construction for the first two datasets, but for the last dataset, both the brute-force method and the algorithm by *Hacid et al.* are impractical to run on a dataset of such size. The accuracy of *Rayar et al.* in this case is found by comparing to our method. The last 100 data points are reserved as a test set for search.

dataset	Algorithm	Total Links	Extra (+) & Missing (-) Links	Average Degree	Search Distances	Index Construction Distances
Corel $N = 68k$	<i>Hacid et al.</i>	212,211	+21,802/-4	6.2378	177,972.36	9,823,840,198,726
	<i>Rayar et al.</i>	190,908	+535/-40	5.6116	169,575.08	6,432,673,175
	Ours	190,413	+0/-0	5.5971	43,729.20	1,611,369,217
MNIST $N = 60k$	<i>Hacid et al.</i>	118,248	+3,778/-3	3.9416	87,713.10	1,430,022,984,523
	<i>Rayar et al.</i>	114,893	+865/-445	3.8298	88,172.04	2,639,416,420
	Ours	114,473	+0/-0	3.8158	10,058.90	407,689,553
LA $N = 1M$	<i>Hacid et al.</i>	Impractical				
	<i>Rayar et al.</i>	1,277,369	+3,254/-33,706	2.3793	2,147,498.42	1,153,035,099,784
	Ours	1,307,821	-	2.4360	1,020.71	1,042,175,220

- Dong, W., Moses, C., Li, K.: Efficient k-nearest neighbor graph construction for generic similarity measures. In: Proceedings of the 20th international conference on World wide web. pp. 577–586 (2011)
- Escalante, O., Pérez, T., Solano, J., Stojmenovic, I.: RNG-based searching and broadcasting algorithms over internet graphs and peer-to-peer computing systems. In: The 3rd ACS/IEEE Int. Conf. on Comp. Systems & App. p. 17. IEEE (2005)
- Fu, C., Xiang, C., Wang, C., Cai, D.: Fast approximate nearest neighbor search with the navigating spreading-out graph. Proceedings of the VLDB Endowment **12**(5), 461–474 (2019)
- Gabriel, K.R., Sokal, R.R.: A new statistical approach to geographic variation analysis. Systematic Zoology **18**(3), 259–278 (1969)
- Goto, M., Ishida, R., Uchida, S.: Preselection of support vector candidates by relative neighborhood graph for large-scale character recognition. In: 2015 13th Int. Conf. on Document Analysis & Recog. (ICDAR). pp. 306–310 (2015)
- Hacid, H., Yoshida, T.: Incremental neighborhood graphs construction for multidimensional databases indexing. In: Conference of the Canadian Society for Computational Studies of Intelligence. pp. 405–416. Springer (2007)
- Han, D., Han, C., Yang, Y., Liu, Y., Mao, W.: Pre-extracting method for svm classification based on the non-parametric k-nn rule. In: 2008 19th International Conference on Pattern Recognition. pp. 1–4. IEEE (2008)
- Jaromczyk, J.W., Toussaint, G.T.: Relative neighborhood graphs and their relatives. Proceedings of the IEEE **80**(9), 1502–1517 (1992)
- Katajainen, J., Nevalainen, O., Teuhola, J.: A linear expected-time algorithm for computing planar relative neighbourhood graphs. Information processing letters **25**(2), 77–86 (1987)
- Kirkpatrick, D.G., Radke, J.D.: A framework for computational morphology. In: Machine Intelligence and Pattern Recognition, vol. 2, pp. 217–248. Elsevier (1985)
- Rayar, F., Barrat, S., Bouali, F., Venturini, G.: An approximate proximity graph incremental construction for large image collections indexing. In: International Symposium on Methodologies for Intelligent Systems. pp. 59–68. Springer (2015)
- Rayar, F., Barrat, S., Bouali, F., Venturini, G.: Incremental hierarchical indexing and visualisation of large image collections. In: 24th European Symposium on Artificial Neural Networks, Computational Intelligence and Machine Learning (2016)

16. Rayar, F., Barrat, S., Bouali, F., Venturini, G.: A viewable indexing structure for the interactive exploration of dynamic and large image collections. *ACM Transactions on Knowledge Discovery from Data (TKDD)* **12**(1), 1–26 (2018)
17. Rayar, F., Goto, M., Uchida, S.: Cnn training with graph-based sample preselection: application to handwritten character recognition. In: 2018 13th IAPR International Workshop on Document Analysis Systems (DAS). pp. 19–24. IEEE (2018)
18. Supowit, K.J.: The relative neighborhood graph, with an application to minimum spanning trees. *Journal of the ACM (JACM)* **30**(3), 428–448 (1983)
19. Tellez, E.S., Ruiz, G., Chavez, E., Graff, M.: Local search methods for fast near neighbor search. *arXiv preprint arXiv:1705.10351* (2017)
20. Toussaint, G.T.: The relative neighbourhood graph of a finite planar set. *Pattern Recognition* **12**(4), 261 – 268 (1980)
21. de Vries, N.J., Arefin, A.S., Mathieson, L., Lucas, B., Moscato, P.: Relative neighborhood graphs uncover the dynamics of social media engagement. In: *Int. Conf. on Advanced Data Mining and App.* pp. 283–297 (2016)